International Journal of Pharmaceutics 397 (2010) 27–35

Contents lists available at ScienceDirect

International Journal of Pharmaceutics

journal homepage: www.elsevier.com/locate/ijpharm

Magnetic resonance imaging and relaxometry to study water transport mechanisms in a commercially available gastrointestinal therapeutic system (GITS) tablet

Amber L. Broadbent[a], Rob J. Fell[a], Sarah L. Codd[b,*], Kim A. Lightley[c], Sanjay Konagurthu[c], Dory G. Koehler-King[c], Joseph D. Seymour[a]

[a] Department of Chemical and Biological Engineering, Montana State University, 306 Cobleigh Hall, Bozeman, MT 59717 USA
[b] Department of Mechanical Engineering, Montana State University, P.O. Box 173800, 220 Roberts Hall, Bozeman, MT 59717 USA
[c] Bend Research, Inc., 64550 Research Road, Bend, OR 97701 USA

ARTICLE INFO

Article history:
Received 25 March 2010
Received in revised form 4 June 2010
Accepted 22 June 2010
Available online 31 July 2010

Keywords:
Controlled-release
Drug delivery
Diffusion
Osmotic pressure
Magnetic resonance imaging
Relaxometry

ABSTRACT

The hydration of 4 mg Cardura XL (Pfizer™), a commercially available gastrointestinal therapeutic system (GITS) tablet, was investigated using magnetic resonance imaging (MRI). A short echo time (T_e = 2.81 ms) technique for MRI of the hydration of a GITS tablet was implemented. From the MR images, signal intensity profiles were generated and interpreted in the context of diffusive and osmotic transport mechanisms. A distinct transition from diffusive to osmotic transport was measured at a timescale relevant to the measured drug release time. Diffusion and osmotic rate coefficients for water in the drug and polymer sweller layers of the tablet were quantified. Spin–lattice T_1 and spin–spin T_2 relaxation times of the water signal from within the tablet were measured as a function of hydration time in order to incorporate the effects of relaxation into interpretation of signal intensity and provide unique information on the distribution of water in different physical and chemical environments within the tablet.

1. Introduction

Gastrointestinal therapeutic system (GITS) tablets utilize osmotic pressure and polymer swelling to deliver active pharmaceutical ingredients in a controlled, steady and reproducible manner. Typically, these tablets consist of two osmotic layers – a drug layer and a water-swellable polymer layer, which are compressed to form a tablet core. The core is coated with a hard cellulosic membrane that is permeable to water but impermeable to ions, the drug and osmotic excipients. The coating contains one or more delivery ports through which the swelling polymer layer "pumps" out a drug suspension after sufficient tablet hydration. The first osmotic pump system which was commercialized for oral drug delivery was developed by Felix Theeuwes in the mid-1970s (Theeuwes, 1975). Since that time, a variety of osmotically controlled oral drug delivery systems have been developed, and these form a major segment of drug delivery products today (Verma et al., 2000; Cardinal, 2000).

In vitro and *in vivo* drug release (dissolution) testing are probably the most common analytical methods for characterizing the performance of pharmaceutical tablets. Other common methods of characterizing the performance of controlled-release (CR) dosage forms include infrared (IR) spectroscopy, differential scanning calorimetry (DSC), and X-ray diffractometry (XRD). These methods can provide information about the physiochemical behaviors of both the active pharmaceutical ingredient (API) and the excipients of a formulation, and may help to identify processing constraints and how the excipients affect drug release and tablet performance. However, these methods provide no direct information about the microstructural changes within the tablet or the transport mechanisms that may be impeding or promoting drug release.

Confocal laser scanning microscopy (CLSM) has been used to study particle deformation during tablet compression (Guo et al., 1999) and to measure the distribution of drug within solid dosage forms during hydration (Cutts et al., 1996). Albeit non-invasive, CLSM requires that the material being probed be fluorescent and therefore requires a model fluorescent sample in place of the true dosage form.

The standard analytical methods for characterizing tablets do not directly provide information on the morphological and com-

* Corresponding author. Tel.: +1 406 994 1944; fax: +1 406 994 6292.
E-mail addresses: amber.broadbent@coe.montana.edu (A.L. Broadbent), fell@nmr.mgh.harvard.edu (R.J. Fell), scodd@coe.montana.edu (S.L. Codd), kim.lightley@bendres.com (K.A. Lightley), sanjay.konagurthu@bendres.com (S. Konagurthu), koehler-king@bendres.com (D.G. Koehler-King), jseymour@coe.montana.edu (J.D. Seymour).

0378-5173/$ – see front matter © 2010 Elsevier B.V. All rights reserved.
doi:10.1016/j.ijpharm.2010.06.047

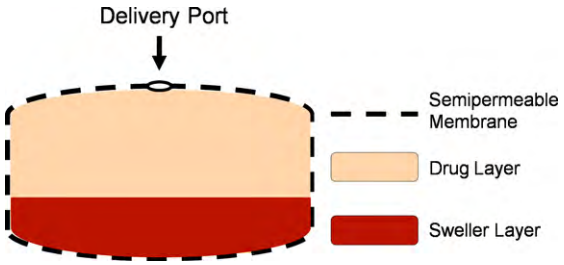

Fig. 1. Cross-section of an osmotic bilayer gastrointestinal therapeutic system (GITS) tablet.

positional changes in the tablet that occur during the drug release process. In order to efficiently formulate and optimize CR dosage forms, an analytical method which non-invasively permits the *in situ* measurement of the microstructural changes which occur during tablet hydration, swelling and drug release in a real (not an altered model) system would be extremely useful.

Magnetic resonance imaging (MRI) is a non-invasive method which does not require a "model" sample. ^{1}H MRI can measure water concentration if the T_2 times of the water are longer than the echo time of the MRI sequence and if all other protons in the sample, *i.e.* protons that are not from water molecules, have much shorter T_2 times, as is the case in the sample used for this study. Therefore, the MRI techniques used here provide spatially resolved images of the penetration of water into the tablet with resolution on the order of hundreds of microns.

Nuclear magnetic resonance (NMR) and MRI have previously been used for pharmaceutically relevant applications to study the hydration of polymers such as hydrogel formation and polymer swelling (Fyfe and Blazek, 1997; Bowtell et al., 1994; Tritt-Goc and Kowalczuk, 2005; Dahlberg et al., 2007), the diffusion and kinetics of water uptake in tablets (Melia et al., 1998; Baille et al., 2002; Malveau et al., 2002; Therien-Aubin et al., 2005) and the microstructural transformation in degradable bioceramics (Bray et al., 2007). MR imaging of tablets in deuterated dissolution media has been used to follow drug solubilization and release and/or the spatial distribution and dynamics of protonated excipients (Black et al., 1998; Dahlberg et al., 2007). MRI was used to qualitatively evaluate GITS tablets which showed different release patterns of drug during quality control testing (Shapiro et al., 1996) and recently a benchtop-MRI system was used to characterize and compare various formulations for Isradipine push–pull tablets (Malaterre et al., 2009). In this work, these studies have been extended to quantify the transition from diffusive to osmotic transport.

2. Materials and methods

Commercially available 4 mg Cardura XL (Pfizer^{TM}) GITS tablets were used for the study. These bilayer osmotic tablets are often referred to as "push–pull" tablets and consist of a drug-containing (Doxazosin Mesylate) "pull" layer and an osmotic water-swellable polymer "push" layer. The solubility of doxazosin at 25 °C is 0.008 g/100 g water (Niazi, 2004). The Cardura XL GITS tablets used here contained the strong osmotic agent, NaCl, in the sweller layer. The layers are bonded together through tablet compression to form a single tablet-shaped core which is enclosed by a semipermeable coating with a single laser-drilled delivery port as depicted in Fig. 1. The Cardura XL tablets used are approximately 9 mm in diameter and 5 mm thick and have mass 290–300 mg.

Deionized water was used to hydrate the tablet. When a GITS Cardura XL tablet is placed in an aqueous environment, due to the presence of osmotic excipients in both of the tablet's layers, diffusive and osmotic processes transport water into the tablet. A suspension of the poorly water soluble drug and excipients forms in the drug layer while the water swellable polymer in the "push" layer begins to expand. As the "push" layer expands, the drug suspension is released through the delivery orifice (Chung et al., 1999). The highly engineered GITS tablet releases drug at an approximately steady rate for 12–18 h under physiological conditions (Fig. 3).

2.1. Dissolution (drug release) studies

The release rate of doxazosin mesylate was determined by using a USP Apparatus II dissolution apparatus with a paddle rotation rate of 75 rpm. Dissolution was performed using standard physiologic conditions as well as the conditions at which the MR imaging experiments were conducted.

The dissolution medium was either de-aerated simulated gastric fluid (SGF), without enzyme, at pH 1.2 and 37 °C (standard conditions), SGF without enzyme, at pH 1.2 and 20 °C or deionized water (DI H_2O) at 20 °C (MR imaging conditions). The sample aliquots were quantified using HPLC with spectrophotometric detection. Preparation for the dissolution test began by adjusting the paddle height to 2.5 ± 0.2 cm from the bottom of the vessels as required by the USP. Dissolution medium was placed into the dissolution vessel and the temperature was equilibrated to the specified temperature. With paddles rotating, placement of one previously weighed tablet was made into the dissolution vessel. An automated sampling system was used to collect samples at pre-determined times. A 10 μm full flow filter was fitted to the sample sippers, and the sampler was programmed to withdraw 1-mL at each time point. Time points of 1, 2, 3, 4, 5, 6, 7, 8, 12 and 18 h were collected. The doxazosin concentration was analyzed for each time point. The results are shown in Fig. 3.

2.2. Magnetic resonance imaging studies

Deionized water at ambient temperature, 20 °C, was used as the dissolution media for these initial MR imaging studies in order to prevent complicating image interpretation with the presence of salts, sugars, etc. Temperature control on the NMR spectrometer currently limits the study to 20 °C.

In ^{1}H MRI experiments the nuclear magnetic moments of hydrogen atoms in a sample are spatially labelled via linearly varying magnetic fields G so that the position of the spins r can be encoded via the precession (Larmor) frequency ω: $\omega(r) = \gamma(B_o + G(r))$ where B_o is the static magnetic field. If the recovery time T_r of the experiment is 1.5 times longer than the spin–lattice relaxation time T_1 of the water inside the GITS tablet and the echo time T_e is chosen to be significantly shorter than the spin–spin relaxation time T_2 of the water in the tablet and longer than the T_2 of any other protons (such as those on polymer excipients) then Fourier transformation of the acquired signal produces a spatial distribution of water density within the tablet. The details of magnetic resonance theory and imaging methods can be found elsewhere (Callaghan, 1991; Blumich, 2005).

The sample was placed in a 500 mL deionized water reservoir to prevent drug saturation of the fluid surrounding the tablet and to accurately reflect the conditions of the dissolution study for comparison. The spectrometer compatible tablet holder and experimental setup are depicted in Fig. 2.

A Bruker Avance III 300 MHz wide vertical bore spectrometer, a 3D gradient coil (1.48 T/m) and a 30 mm ^{1}H probe were used for the imaging studies. The gradient coil temperature was maintained at 20 °C throughout the imaging experiments. A standard slice selective spin-echo sequence with an echo time T_e of 2.81 ms and a recovery time T_r of 1 s were used. Each image consisted of 20 averages obtained over approximately 43 min with a slice thickness of 2 mm and an in-plane resolution of 312 μm × 234 μm.

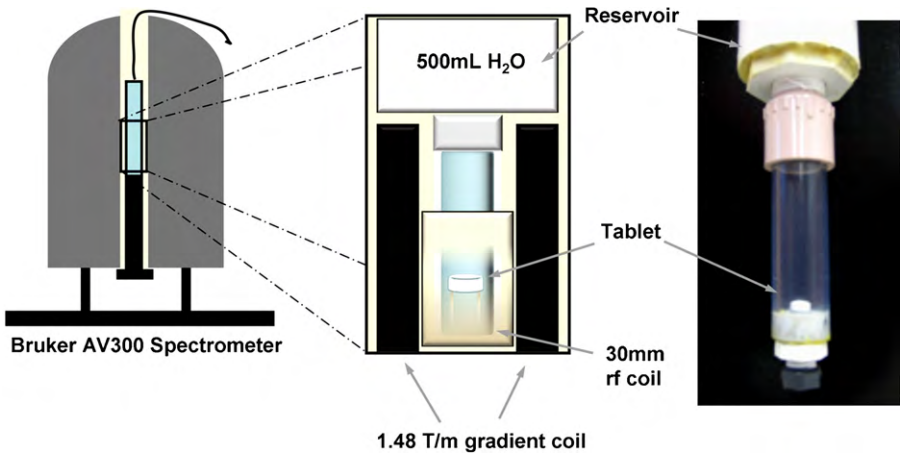

Fig. 2. Experimental setup. The tablet holder is placed in the bore of the Bruker Avance III 300 MHz wide vertical bore spectrometer so that the tablet lies in the active region of the 30 mm radio frequency (rf) coil.

2.3. Magnetic resonance relaxometry studies

Relaxometry studies were conducted in a Bruker DRX 250 MHz vertical bore spectrometer equipped with a 10 mm ^{1}H probe. Tablets were soaked in 500 mL of deionized water on the bench top, then gently dried and placed completely in the active region of the probe. A Carr–Purcell–Meiboom–Gill (CPMG) (Carr and Purcell, 1954) one-dimensional pulse sequence and Laplace inversion (Godefroy and Callaghan, 2003) were used to determine the distribution of T_2 relaxation times present in the tablets for a range of hydration times. The T_1 relaxation times of the tablets were determined using a 90° pulse experiment to determine the T_r at which full signal recovery had occurred.

2.4. Transport modeling

For this study, the simplest transport model was chosen to reflect the order of magnitude of the diffusivities, and in particular, elucidate differences in timescales and identify when changes in the mechanism of transport occurs. A one-dimensional mass conservation model was used in order to identify the dominant transport mechanisms and to estimate effective transport coefficients for flux of water into the GITS tablet. This simple transport model was chosen because GITS tablets have been shown to have zero-order release kinetics and are minimally affected by environmental factors such as pH or convection (Conley et al., 2006; Theeuwes, 1975). Specifically, doxazosin GITS tablets have been shown to perform independently of stir rate in the range of 50–100 rpm and are unaffected by pH in the range of 1.2–7.5 (Chung et al., 1999).

Approximating the 3D tablet as a 1D rod is the first step in showing the significant data MR images can provide regarding the transport mechanisms in real tablet systems. The 1D mass conservation transport equation is

$$\frac{\partial c}{\partial t} = D\frac{\partial^2 c}{\partial x^2} + \frac{N}{l}. \tag{1}$$

The transport has been broken into two mechanisms: molecular diffusion with effective diffusivity D and osmotic pressure driven flux, $N = K\Delta\pi$. The osmotic flux occurs across a membrane of thickness l and with permeability coefficient K considering only the osmotic pressure driving force $\Delta\pi$ (Mccabe et al., 2005).

Solving Eq. (1) with $D(\partial^2 c/\partial x^2) \gg (N/l)$, the diffusion dominated transport regime, and subject to the initial condition $c(x,0) = f(x)$ where $\begin{matrix} f(x) = 1, & x \le 0 \text{ or } x \ge L \\ f(x) = 0, & 0 < x < L \end{matrix}$ and boundary conditions $c(0,t) = c(L,t) = 1$ for a rod of length L results in the Fourier series solution,

$$c(x,t) = 1 + \sum_{n=1}^{\infty} \frac{2}{n\pi}(\cos(n\pi) - 1)\sin\left(\frac{n\pi x}{L}\right) e^{-(Dn^2\pi^2 t/L^2)} \tag{2}$$

Eq. (2) can be fit to the experimentally obtained $c(x,t)$, *i.e.* normalized signal intensity, and D can be determined.

In the osmotic pressure dominated transport regime $(N/l) \gg D(\partial^2 c/\partial x^2)$, the osmotic pressure driving force can be approximated using Van't Hoff's Law (Fournier, 1999),

$$\Delta\pi = \frac{RT}{V_w^l} \ln(\gamma_w x_w) = -\frac{RT}{V_w^l} x_s \tag{3}$$

where R is the ideal gas constant, T is temperature, V_w^l is the molar specific water volume, x_w is the mole fraction of water and γ_w is the water activity coefficient. For a dilute ideal solution approximation, the osmotic pressure is related to x_s the mole fraction of solute in the tablet sweller layer. Substituting $x_s = 1 - x_w$ into Eq. (3) enables $\Delta\pi$ to be written in terms of normalized water concentration c,

$$\Delta\pi = -\frac{RT}{V_w^l}(1 - x_w) \sim -\frac{RT}{V_w^l} + RTc \tag{4}$$

Plugging this relation into Eq. (1) for negligible diffusive transport generates a solution of the form $c(t) = c_o e^{\beta t}$ with $\beta = KRT/l$.

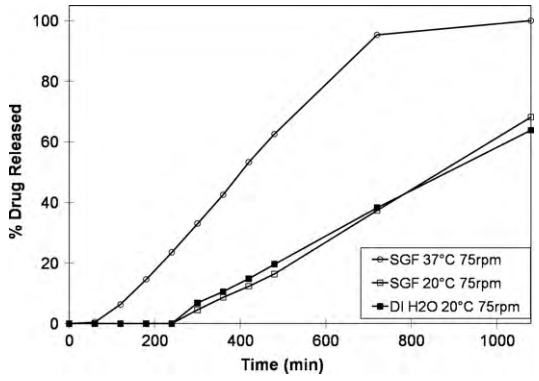

Fig. 3. Drug release profiles obtained using standard dissolution conditions (SGF, 37 °C) and using the conditions present in the MR imaging experiments (DI H_2O, 20 °C). The drug release profile obtained using SGF at 20 °C shows that the difference in the MR imaging conditions profile from the standard dissolution conditions profile is due to the effects of temperature on diffusion rates. The paddle mixing rate was maintained at 75 rpm for all dissolution studies in order to prevent inaccurate drug release measurements. MR images were obtained under stagnant conditions, without mixing.

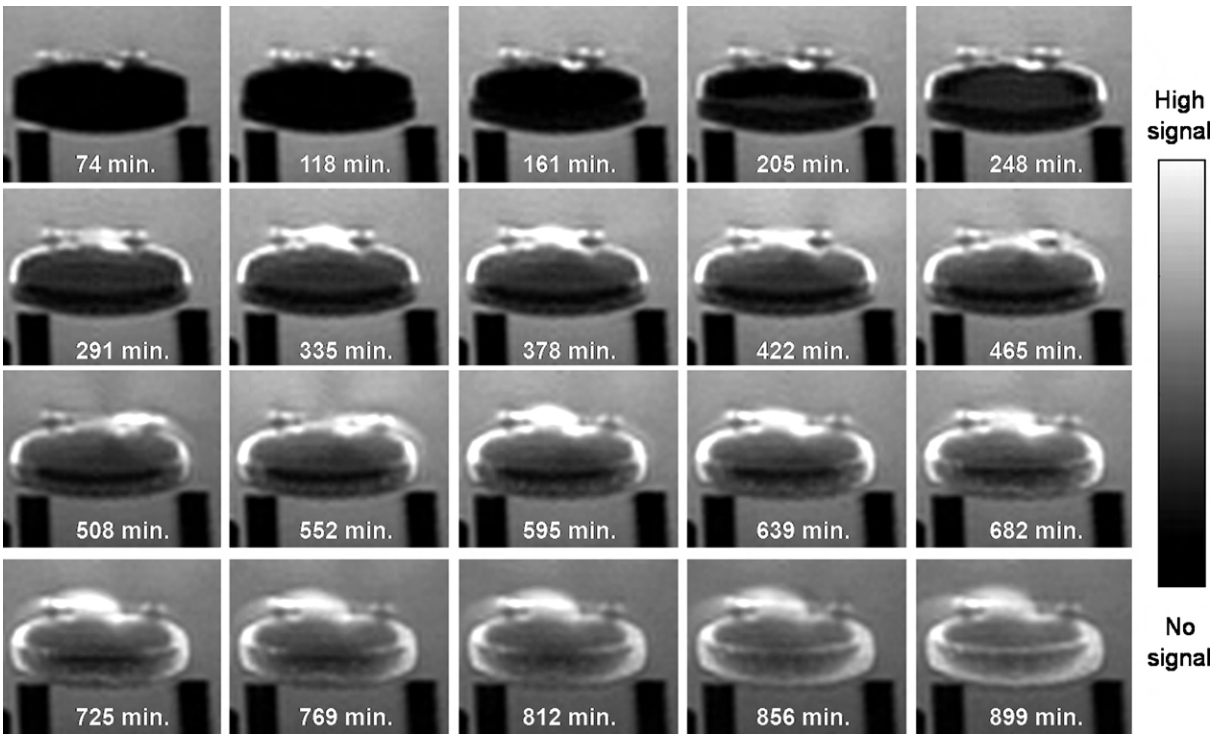

Fig. 4. Images of the trial 3 Cardura XL tablet over a 16-h time period. The signal intensity for each image is averaged over a 43 min time period. The gradual increase in signal intensity inside the tablet is due to tablet hydration. The hydration of the sweller layer causes it to swell, pushing the drug suspension into the surrounding dissolution fluid through the laser-cut orifice at the top of the membrane. A spin echo sequence with T_r = 1 s, T_e = 2.81 ms, slice thickness = 2 mm and in plane resolution = 312 μm × 234 μm was used for all images.

3. Results and discussion

3.1. Dissolution profile

Dissolution studies (Fig. 3) showed that the time required for 100% drug release under standard dissolution conditions is approximately 12–18 h. During the drug delivery process, the drug is released at an approximately constant (apparent zero order) rate through the single delivery port at the top of the tablet. Using the MR imaging experimental conditions (DI H_2O, 20 °C) for dissolution testing resulted in 65% drug released after 18 h. The drug release profile obtained using SGF at 20 °C, shows that the difference in the release profiles is due to the effects of temperature on diffusion rates (Bird et al., 2002). As expected, drug release was found to be independent of the dissolution media used (Chung et al., 1999). The dissolution performance of the

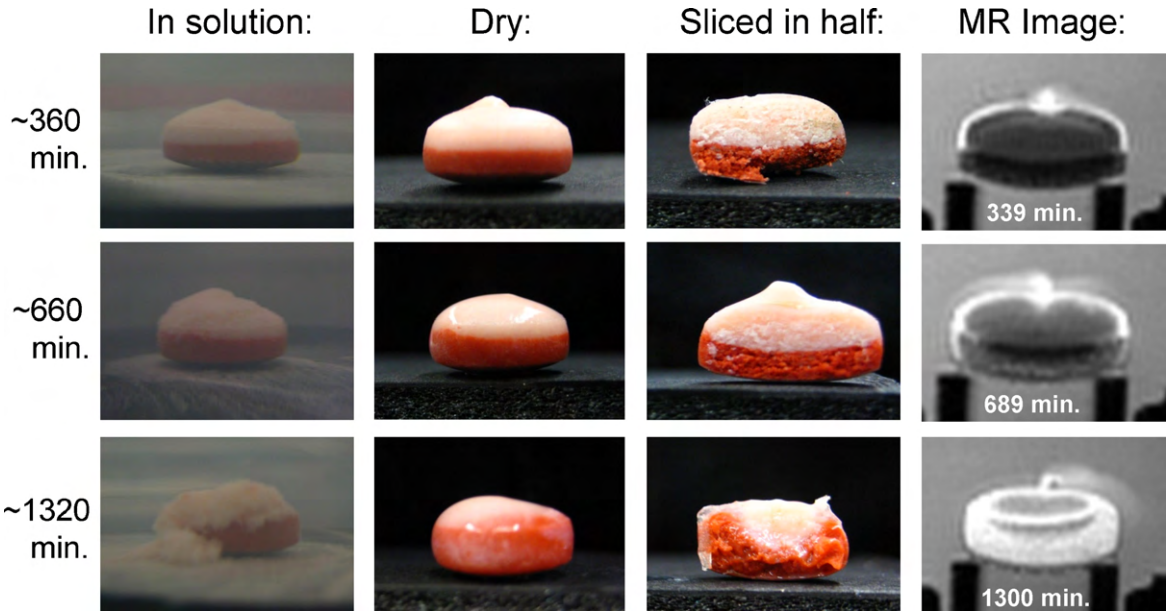

Fig. 5. Comparison of the trial 1 Cardura XL tablet MR images (far right) to digital images of a tablet (in 500 mL of deionized water in a glass beaker) corresponding to the same soaking times. Images from left to right: tablet soaking in beaker of water; tablet after removing it from the water; cross-section of tablet after slicing it in half longitudinally; MR image of tablet placed in MR tablet holder at corresponding hydration time. Corresponding features in the images include the drug suspension deposited on the upper surface of the tablet, clear distinction between the drug and sweller layers, and swelling of the sweller layer.

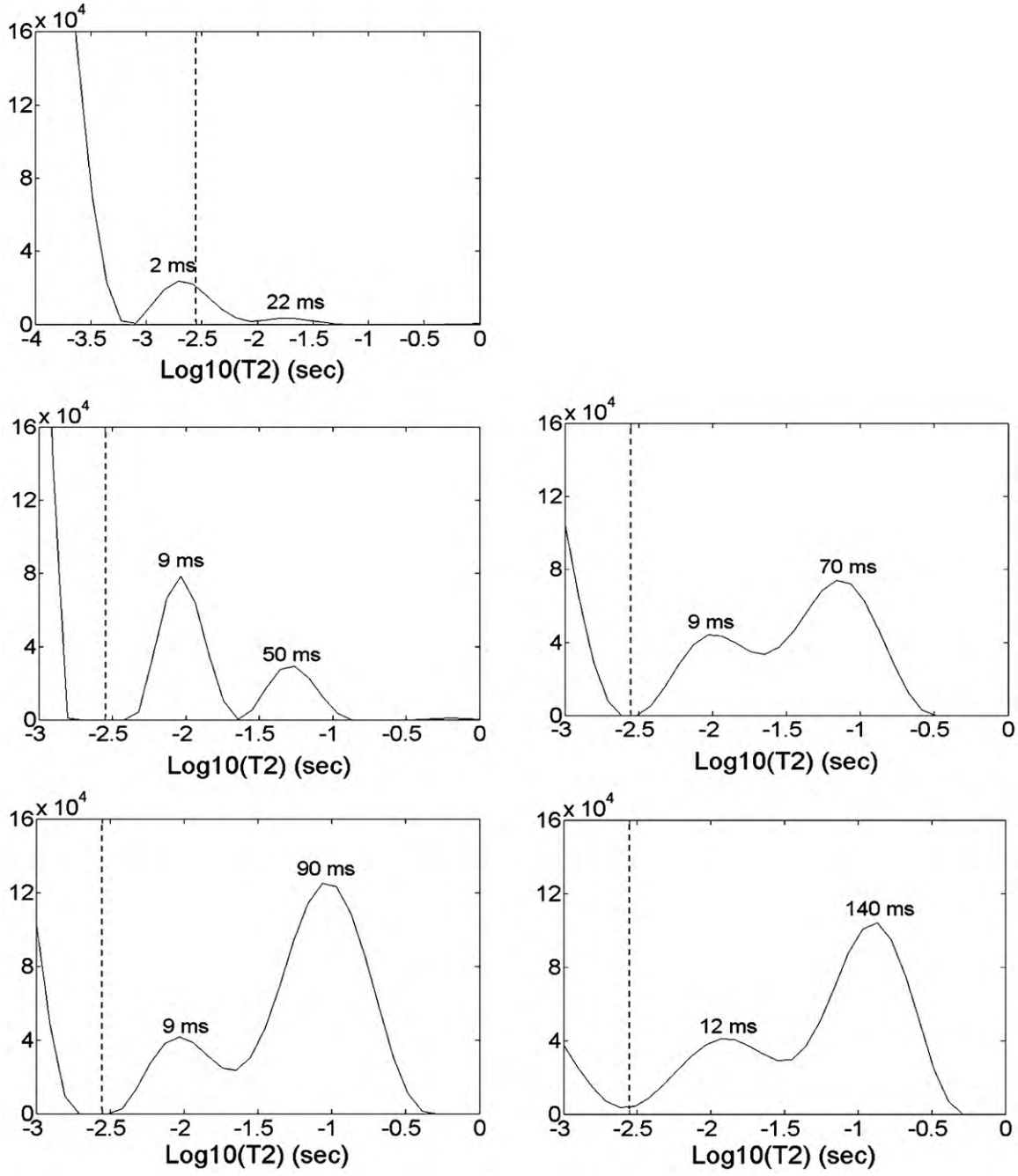

Fig. 6. Log scale T_2 relaxation time distributions in the Cardura XL tablet (a) dry and at hydration times (b) 1 h (c) 4 h (d) 8 h and (e) 16 h. The dashed line in each distribution marks the 2.81 ms echo time used in the 2D MR imaging experiments.

tablets was found to be extremely reproducible under all conditions tested.

3.2. MR images

Three separate experiments on different tablets (trials) were conducted over a 16 h time period. The results from 'trial 3' are shown in Fig. 4. The 'trial 3' images were selected because this trial had the best time resolution of 20 images taken over the 16 h time period. The images for all trials are similar as reflected in the subsequent data analysis and transport modeling which incorporates data from all three trials.

The T_1 relaxation of the bulk water ($T_{1\text{bulk}} \geq 3$ s) surrounding the tablet is longer than the experiment T_r of 1 s. Therefore in that region the image intensity does not directly reflect water density as it is T_1-weighted and hence the observed signal intensity is lower than in regions of the tablet with $T_1 \ll T_r$, which do accurately represent water density.

In Fig. 5 the MR images taken at three different times (339, 689 1300 min) are compared to the optical images of GITS tablets soaked for the corresponding time period. Within the tablet layers, the MR images show an increase in signal intensity over time due to increasing water concentration within the tablet as it hydrates.

3.3. Relaxation times and the impact on imaging

In order to use the MR images to investigate water transport in the drug and sweller layers of the tablet, it is necessary to determine

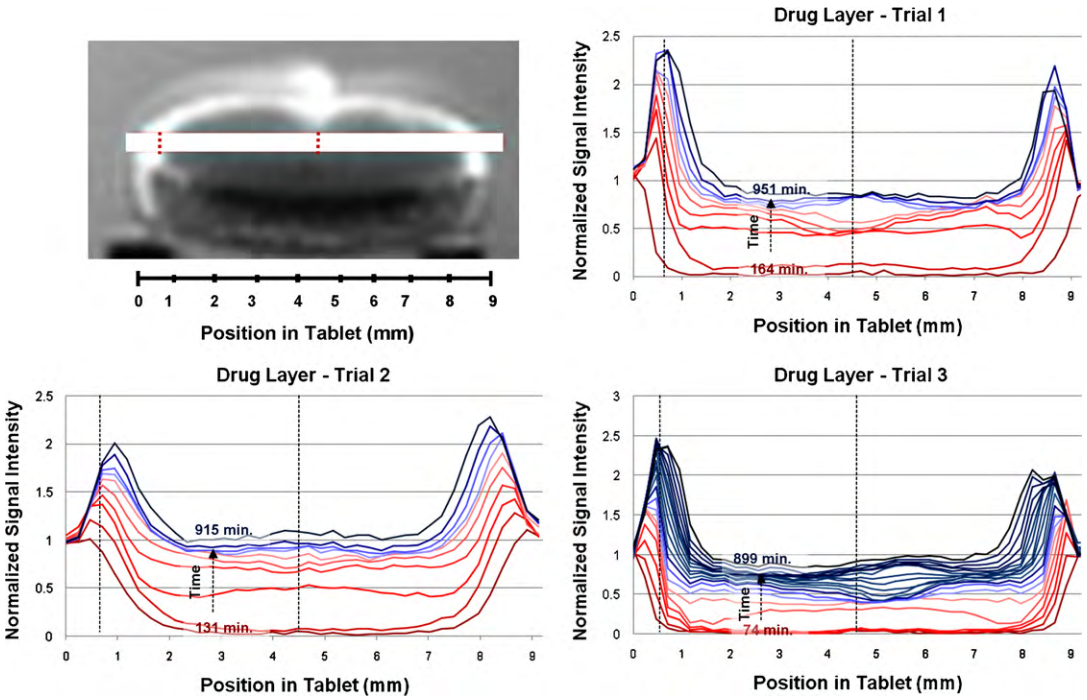

Fig. 7. Signal intensity profiles for the drug layers for each of the three trials show similar behavior. Each line of data corresponds to the line through the drug layer (top left) for each image, or time point. The dashed line at position 4.5 mm corresponds to the data analyses shown in Fig. 10. Note the signal intensity variation with time in the membrane, dashed line at position 0.7 mm.

that the image intensities accurately reflect water concentration in these regions. A study of the relaxation times, T_2 and T_1, in the tablet throughout the 16 h hydration period allowed a high degree of confidence that this was the case.

In Fig. 6, distributions of T_2 relaxation times are presented for tablets hydrated for 1, 4, 8 and 16 h. For all hydration times, the two primary measured relaxation populations are at approximately 10 ms and greater than 40 ms. We currently interpret these distinct populations as belonging to distinct regions in space, within which the spins could be in fast exchange with the rigid polymers in that region. The very short T_2 signal, *i.e.* fast T_2 relaxation time (<1 ms) is from protons located on the rigid polymer molecules of the tablet,

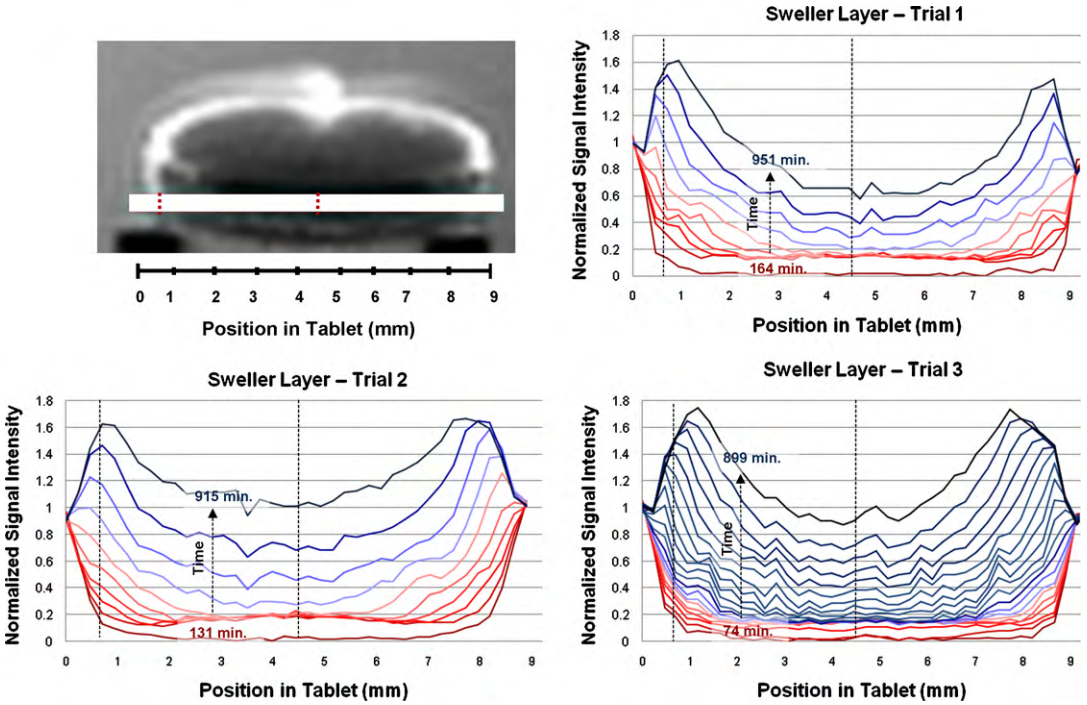

Fig. 8. Signal intensity profiles for the sweller layers for each of the three trials show similar behavior. Each line of data corresponds to the line through the sweller layer (top left) for each image, or time point. The dashed line at position 4.5 mm corresponds to the data analysis shown in Fig. 11. Note the signal intensity variation with time in the membrane, dashed line at position 0.7 mm.

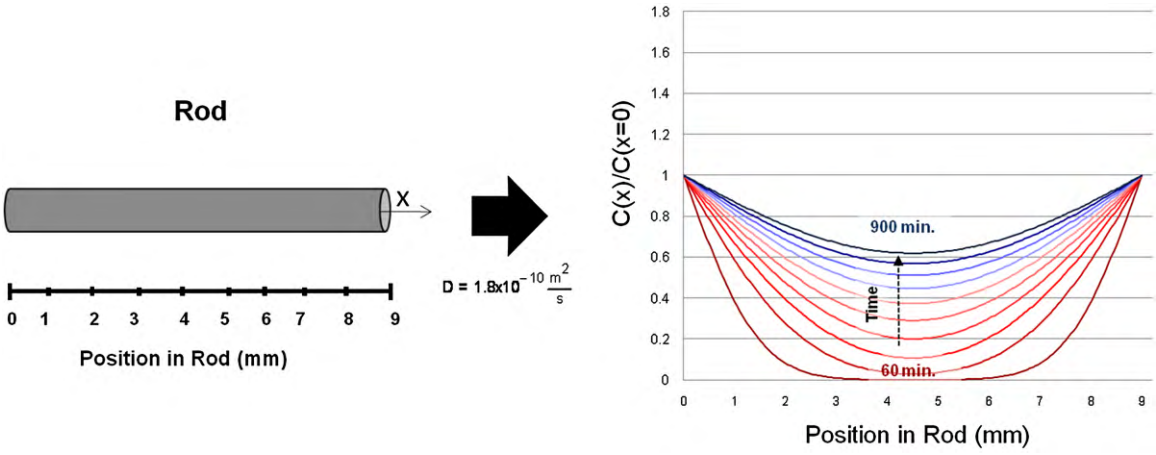

Fig. 9. The model signal intensity profile was generated using the 1D diffusion model (Eq. (2)) for a time period of 60–900 min. The model provides a basis with which to interpret the diffusive behavior of the osmotic GITS tablets and to estimate effective diffusivity of water within the drug and sweller layers.

as evidenced by measurement of the T_2 distribution of a dry tablet, and these protons will therefore not contribute to the image signal acquired using a T_e of 2.81 ms, but they will influence the T_2 of the water due to the fast exchange with the surrounding water. As a specific region is hydrated then the relative population exchange between the relaxation sites on the polymers will decrease and the relaxation time of water in that region will increase.

The very short T_2 signal, (<1 ms) will not contribute to the image signal acquired using a T_e of 2.81 ms.

Between the 1 h (60 min) and 4 h (240 min) hydration time points, the short T_2 (~9 ms) population broadens and yet remains approximately constant in net area. However, the longer T_2 relaxation time population significantly increases in area. Based on the images in Fig. 4, the longer T_2 relaxation time population is the water in the drug layer as this is the region where signal increases in the images during the first 4 h.

Between the 4 h (240 min) and 8 h (480 min) hydration times, the net area associated with the longer T_2 relaxation time population remains fairly constant. Referencing the images of Fig. 4, the drug layer signal remains fairly constant between 4 h (240 min) and 8 h (480 min), which provides additional support for the conclusion that the longer T_2 relaxation time population is the water within the drug layer.

For all the T_2 values present, the 2.81 ms echo time used in the MR images would result in no T_2-weighting in the drug layer and only slight T_2-weighting in the sweller layer.

Understanding whether T_1-weighting is occurring within the tablet region of the MR images with a $T_r = 1$ s is important as it is assumed for subsequent analysis and modeling that the signal intensity in the tablet reflects water concentration. The approximate T_r at which signal intensity remained steady for free water was approximately 5 s, so there is definitely T_1-weighting in this region. However, this is of no concern as we do not need to measure water concentration in the surrounding bulk water. For a tablet hydrated for 1 h, $T_1 \approx 600$ ms and for a tablet hydrated for 8–16 h, $T_1 \approx 200$ ms. This analysis indicates that a small amount of T_1-weighting of the signal from within the tablet was present at early times in the tablet imaging studies, but that T_1-weighting was not significant at hydration times beyond 6 h. The longer T_1 at early hydration times is probably due to the heavier weighting of the overall tablet signal by the polymer which will have long T_1 values. Therefore, the T_1-weighting of the water is likely to be even less than the small amount these values suggest, indicating a direct correlation between signal intensity and water concentration is valid.

3.4. Estimating effective diffusion and the rate of osmotic transport

For each image acquired over the 16-h hydration time, signal intensity data for a 624 μm wide and 9 mm long horizontal region was selected from each layer of the tablet (top left image in Figs. 7 and 8). The signal intensity data for each image, *i.e.* time point, was normalized to the average signal intensity of the surrounding water, as it was assumed that the T_1-weighting of the bulk water was stable over the duration of the experiment. The plots of spatially and temporally varying signal intensity reveal the transport behavior of water in the drug (Fig. 7) and the sweller (Fig. 8) layers. The signal intensity profiles for each of the three trials show the same behavior.

The 1D time-dependent diffusive model Eq. (2) yields the concentration profiles shown in Fig. 9 for a diffusivity value of $D = 1.8 \times 10^{-10}$ m^2/s. For reference, the free diffusivity of water at 20 °C is 2.2×10^{-9} m^2/s (Mills, 1973).

Signal intensity for a region (area = 624 μm × 234 μm) located in the center of each layer of the tablet (dashed lines located at $x = 4.5$ mm in Figs. 7 and 8) was used to estimate the effective diffusivity of water in both the drug (Fig. 10) and sweller (Fig. 11)

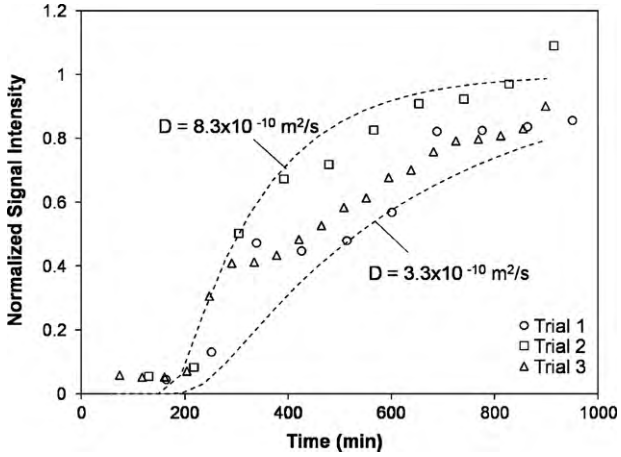

Fig. 10. Diffusive transport in the drug layer. The data shown is taken from a pixel (area: 624 μm × 234 μm) in the center of the drug layer (dashed line at 4.5 mm in Fig. 7). Comparing this behavior to the diffusion model (dashed lines), the diffusivity for the water moving into the drug layer appears to lie in the range of $D = 3.3 \times 10^{-10}$ m^2/s to $D = 8.3 \times 10^{-10}$ m^2/s.

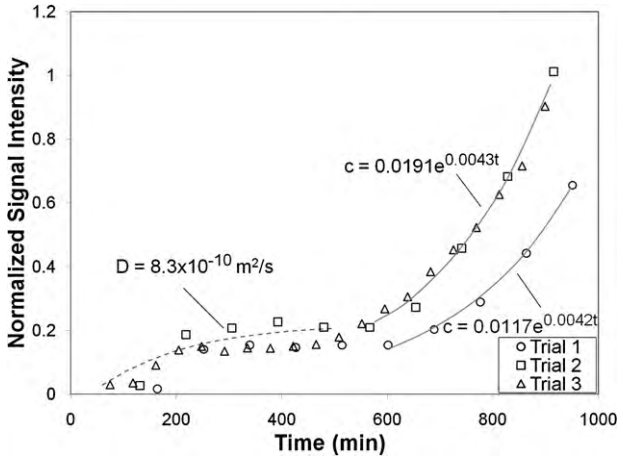

Fig. 11. Diffusive and osmotic transport in the sweller layer. The data shown is taken from a single pixel in the center of the sweller layer (dashed line at 4.5 mm in Fig. 8). There appears to be a hydration "lag time" after ~200 min for each trial. Comparing the initial hydration behavior to the diffusion model (dashed line), the diffusivity for the water moving into the polymer sweller layer during the first 600 min appears to lie somewhere around $D = 8.3 \times 10^{-10}$ m^2/s. The sweller layer behavior after $t = 600$ min is non-diffusive and suggests an osmotic transport mechanism. The increase in signal intensity, *i.e.* water concentration, at $t \geq 600$ min was approximated using an exponential model and the equations for the exponential increase in signal intensity are shown.

layers. In the drug layer (Fig. 10) between 200 and 350 min, hydration appears to be rapid, observable by a steep increase in signal intensity after an initial slow hydration regime. For the duration of the MR imaging experiments, the drug layer follows a diffusion process comparable to the generated diffusion model with diffusivity values lying in the order of magnitude $D \approx 3.3 \times 10^{-10}$ m^2/s to $D \approx 8.3 \times 10^{-10}$ m^2/s.

During the initial hydration of the tablet ~600 min (10 h), movement of water into the sweller layer (Fig. 11) exhibits similar behavior to that of the diffusion model with a diffusivity value around $D \approx 8.3 \times 10^{-10}$ m^2/s. From 600 min on, the sweller layer shows a rapid increase in signal intensity that is not consistent with a purely diffusive process. A physical mechanism such as flux increase due to osmotic pressure changes (Malaterre et al., 2009) is indicated. When water first transports into the sweller layer, the driving transport mechanism is the chemical potential difference due to the water concentration gradient (water diffusing into a porous solid). At around $t = 600$ min, enough of the sweller layer matrix is solubilized that the water, polymer and osmotic agent in the sweller layer can be described as a concentrated solution. At this point, as indicated by the exponential increase in the water concentration (see Section 2.4), the driving transport mechanism is the chemical potential due to the osmotic pressure between two different solutions across a membrane. This interpretation is consistent with the increase in the number of molecules in the shorter T_2 relaxation time distribution and the increasing value of T_2 for that distribution (Fig. 6) for times longer than 600 min. As mentioned earlier, the increase in T_2 is consistent with the increase in the rotational mobility of the water and the polymers, and the decrease in the relative population of polymer to water to contribute to proton exchange for the water molecules that occurs as a solution forms.

The data indicates an exponential increase in signal intensity for $t \geq 600$ min. Exponential models approximating the behavior of the water in the sweller layer during this osmosis-dominated mass transport regime are shown in Fig. 11. The rate coefficient $\beta = KRT/l \sim 0.0043$ s^{-1} is similar for all trials. The model's ability to quantify osmotic transport is limited due to the Van't Hoff's Law approximation, which is valid only for low solute concentrations, but clearly shows that osmotic transport is occurring. MR imaging studies in which water transport is limited to one dimension, systematically varying formulation and a more detailed thermodynamic analysis of the osmotic pressure driving force are necessary to fully quantify the diffusive and osmotic transport coefficients.

4. Conclusions

A short echo time ($T_e = 2.81$ ms) MRI technique for imaging the hydration of a GITS tablet was implemented, and three separate imaging trials were conducted. A simple 1D transport model allowed for direct quantification of the transport processes. The data from the three trials was consistent and order of magnitude diffusivity values for water in the drug layer were determined from the 1D diffusion model: 3.3×10^{-10} m^2/s $\leq D_{drug} \leq 8.3 \times 10^{-10}$ m^2/s. Water diffusivity in the sweller layer was 8.3×10^{-10} m^2/s so that the diffusion behavior in both layers appeared similar. The unique nature of the data allowed the clear transition to osmotic transport in the sweller layer to be directly measured. Data and analysis presented here provide important first steps toward development of realistic 3D transport models.

Acknowledgements

The authors acknowledge Mr. Erik M. Rassi for his work constructing the tablet holder and thank Prof. Paul T. Callaghan for providing the Laplace Inversion software used for analyzing the tablet T_2 relaxation time data. RJF acknowledges the support of NIH Grant Number P20 RR016455-04 from the INBRE-BRIN Program of the NCRR NIH. ALB acknowledges the support of Bend Research, Inc. JDS and SLC acknowledge research support from Bend Research, Inc. and NSF and the Murdock Foundation for equipment funding.

References

Baille, W.E., Malveau, C., Zhu, X.X., Machessault, R.H., 2002. NMR imaging of high-amylose starch tablets. 1. Swelling and water uptake. Biomacromolecules 3, 214–218.
Bird, R.B., Stewart, W.E., Lightfoot, E.N., 2002. Transport Phenomena. Wiley & Sons, New York.
Black, N., Vienneau, T., Pan, Y., 1998. NMR microimaging: a useful tool to study the dissolution of solids. In: Blumich, B., Blumler, P., Fukushima, E., Botto, R.E. (Eds.), Spatially Resolved Magnetic Resonance. Wiley-VCH.
Blumich, B., 2005. Essential NMR. Springer-Verlag.
Bowtell, R., Sharp, J.C., Peters, A., Mansfield, P., Rajabi-Siahboomi, A.R., Davies, M.C., Melia, C.D., 1994. NMR microscopy of hydrating hydrophilic matrix pharmaceutical tablets. Magnetic Resonance Imaging 12, 361–364.
Bray, J.M., Petrone, C., Filiaggi, M., Beyea, S.D., 2007. Measurement of fluid ingress into calcium polyphosphate bioceramics using nuclear magnetic resonance microscopy. Solid State Nucl. Magn. Reson. 32, 118–128.
Callaghan, P.T., 1991. Principles of Nuclear Magnetic Resonance Microscopy. Oxford University Press, New York.
Cardinal, J.R., 2000. Controlled release osmotic drug delivery systems for oral applications. In: Amidon, G.L., Lee, P.I., Topp, E.M. (Eds.), Transport Processes in Pharmaceutical Sciences. CRC Press.
Carr, H.Y., Purcell, E.M., 1954. Effects of diffusion on free precession in nuclear magnetic. Phys. Rev. 94, 630–638.
Chung, M., Vashi, V., Puente, J., Sweeney, M., Meredith, P., 1999. Clinical pharmacokinetics of doxazosin in a controlled-release gastrointestinal therapeutic system (GITS) formulation. J. Clin. Pharmacol., 678–687.
Conley, R., Gupta, S.K., Sathyan, G., 2006. Clinical spectrum of the osmotic-controlled release oral delivery system (OROS), an advanced oral delivery form. Curr. Med. Res. Opin. 22, 1879–1892.
Cutts, L.S., Hibberd, S., Adler, J., Davies, M.C., Melia, C.D., 1996. Characterising drug release processes within controlled release dosage forms using the confocal laser scanning microscope. J. Control. Release 42, 115–124.
Dahlberg, C., Fureby, A., Michael, S., Dvinskikh, S.V., Furo, I., 2007. Polymer mobilization and drug release during tablet swelling. A ^{1}H NMR and NMR microimaging study. J. Control. Release 122, 199–205.
Fournier, R.L., 1999. Basic Transport Phenomena in Biomedical Engineering. Taylor & Francis.
Fyfe, C.A., Blazek, A.I., 1997. Investigation of hydrogel formation from hydroxypropylmethylcellulose (HPMC) by NMR Spectroscopy and NMR Imaging Techniques. Macromolecules 30, 6230–6237.

Godefroy, S., Callaghan, P.T., 2003. 2D relaxation/diffusion correlations in porous media. Magn. Reson. Imaging, 21.
Guo, H.X., Heinamaki, J., Yliruusi, J., 1999. Characterization of particle deformation during compression measured by confocal laser scanning microscopy. Int. J. Pharm. 186, 99–108.
Malaterre, V., Metz, H., Ogorka, J., Gurny, R., Loggia, N., Mader, K., 2009. Benchtop-magnetic resonance imaging (BT-MRI) characterization of push–pull osmotic controlled release systems. J. Control. Release 133, 31–36.
Malveau, C., Baille, W.E., Zhu, X.X., Marchessault, R.H., 2002. NMR imaging of high-amylose starch tablets. 2. Effect of tablet size. Biomacromolecules 3, 1249–1254.
Mccabe, W.L., Smith, J.C., Harriott, P., 2005. Unit Operations of Chemical Engineering. McGraw Hill.
Melia, C.D., Rajabi-Siahboomi, A.R., Bowtell, R.W., 1998. Magnetic resonance imaging of controlled release pharmaceutical dosage forms. Pharm. Sci. Technol. Today, 1.
Mills, R., 1973. Self-diffusion in normal and heavy water in the range 1–45°. J. Phys. Chem. 77, 685–688.
Niazi, S., 2004. Handbook of Pharmaceutical Manufacturing Formulations: Compressed Solid Products. Informa Health Care.
Shapiro, M., Jarema, M.A., Gravina, S., 1996. Magnetic resonance imaging of an oral gastrointestinal therapeutic system (GITS) tablet. J. Control. Release 38, 123–127.
Theeuwes, F., 1975. Elementary osmotic pump. J. Pharm. Sci. 64, 1987–1997.
Therien-Aubin, H., Baille, W.E., Zhu, X.X., Marchessault, R.H., 2005. Imaging of high-amylose starch tablets. 3. Initial diffusion and temperature effects. Biomacromolecules 6, 3367–3372.
Tritt-Goc, J., Kowalczuk, J., 2005. Spatially resolved solvent interaction with glassy HPMC polymers studied by magnetic resonance microscopy. Solid State Nucl. Magn. Reson. 28, 250–257.
Verma, R.K., Mishra, B., Garg, S., 2000. Osmotically controlled oral drug delivery. Drug Dev. Ind. Pharm. 26, 695–708.